

Temperature dependence of normal mode reconstructions of protein dynamics

Francesco Piazza and Paolo De Los Rios

Laboratoire de Biophysique Statistique, SB ITP ,
Ecole Polytechnique Fédérale de Lausanne - EPFL, CH-1015, Lausanne, Switzerland

Fabio Cecconi

SMC-INFM Center for Statistical Mechanics and Complexity (CNR) and Istituto dei Sistemi Complessi CNR
Via dei Taurini 19, 00185 Rome, Italy.

(Dated: June 22, 2018)

Normal mode analysis is a widely used technique for reconstructing conformational changes of proteins from the knowledge of native structures. In this Letter, we investigate to what extent normal modes capture the salient features of the dynamics over a range of temperatures from close to $T = 0$ to above unfolding. We show that on the one hand, the use of normal modes at physiological temperatures is justified provided proteins are cooperative. On the other hand, it is imperative to consider several modes in order to eliminate the unpredictable temperature dependence of single-mode contributions to the protein fluctuations.

PACS numbers: 87.15.-v, 87.10.Tf, 87.14.E-

The effectiveness of proteins at performing their functions strongly depends on their ability to dynamically explore different conformations. In many cases, the different functionally relevant conformations correspond to global deformations of the molecules, although not necessarily of large amplitude. In such circumstances, the small-amplitude dynamics can be adequately described through Normal Modes (NM) analysis in order to decipher the structure-dynamics-function relation [1, 2].

NM analysis of macromolecules has a venerable history, dating back to the early 1980's [3, 4], and has enjoyed several renaissances, most prominently in its latest variant, the Anisotropic Network Model and its derivatives [5, 6]. The cornerstone of NM approach is the assumption that functional dynamics of proteins can be captured by the lowest-frequency harmonic normal modes as long as the native-state deformations are of small amplitude. Therefore, the complex potential energy $V(\{\vec{r}\})$ ruling protein dynamics can be expanded, as a function of the atomic coordinates \vec{r}_i , $i = 1, \dots, N$, to second order in the fluctuations around the native state

$$V(\{\vec{r}\}) \simeq \frac{1}{2} \sum_{i,j} \partial_{i\alpha, j\beta}^2 V|_{\vec{R}_i} \Delta r_{i\alpha} \Delta r_{j\beta}, \quad (1)$$

where $\Delta r_{i\alpha} = r_{i\alpha} - R_{i\alpha}$, $R_{i\alpha}$ being the native state coordinates. The dynamical matrix of the system is defined as $D = M^{-1/2} H M^{-1/2}$, with M the diagonal mass matrix and H the Hessian of the potential. The eigenvectors $\hat{\psi}_k$, $k = 1, \dots, 3N$, of D are the normal modes of the protein.

Although NM analysis has been applied with success also to predict large scale deformations, its appropriate context remains the small-amplitude regime and extrapolation to larger fluctuations should be rigorously checked to avoid arbitrary interpretations. In fact, at $T = 300$ K, a mere 10 % below typical protein unfolding tempera-

tures (T_f), displacements well beyond the harmonic approximation must be expected. A possible way to find suitable collective coordinates to describe large fluctuations is to use the “essential modes”, the eigenvectors of the covariance matrix of the displacements from the native state, computed in a molecular dynamics simulation [7]. Unfortunately, the convergence of the covariance matrix toward a stationary solution is very slow [8].

In this Letter, we establish on a firm basis the validity of the NM description of protein dynamics and unveil some remarkable subtle features of this approach as temperature is increased from very low to beyond T_f .

In order to measure the spectral weight of protein fluc-

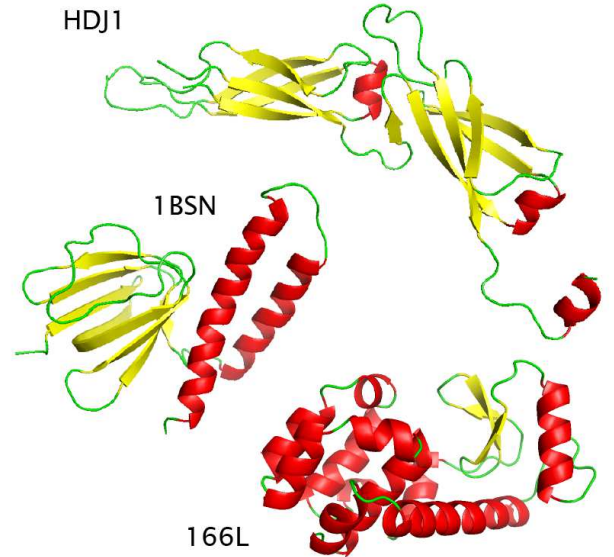


FIG. 1: Cartoon representations of three of the analyzed structures, along with the corresponding PDB codes.

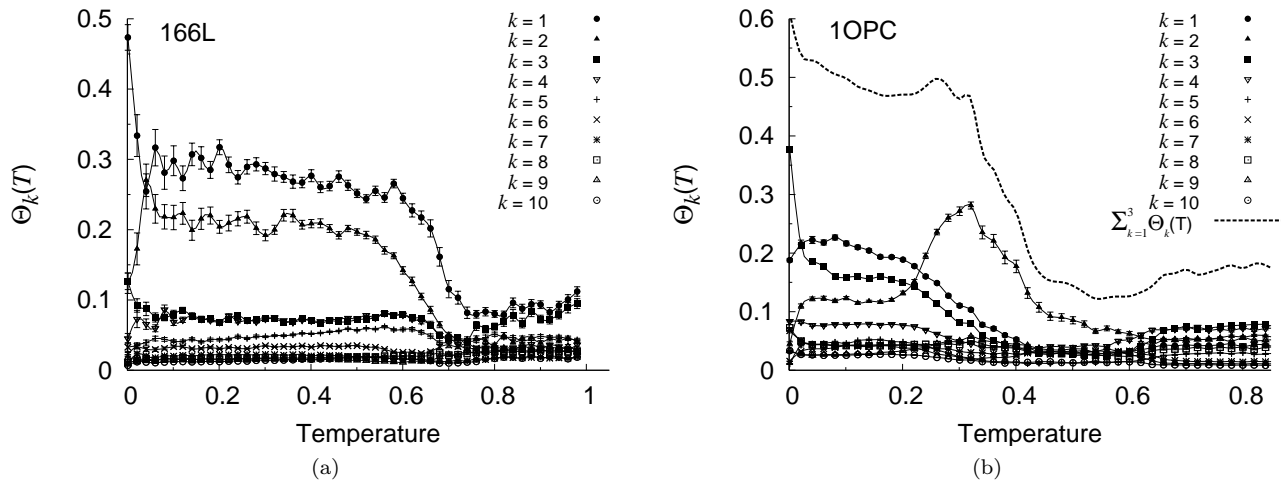


FIG. 2: First ten thermal involvement coefficients of Lysozyme (a), $N = 162$, $T_f = 0.75$, PDB code 166L and of the OMPR DNA-binding domain (b), $N = 99$, $T_f = 0.65$, PDB code 1OPC, as functions of temperature.

tuations as a function of temperature, we introduce the thermal involvement coefficients (TICs) $\Theta_k(T)$ [9]. They are defined as $\Theta_k(T) = \langle Y_k(T) \rangle_{\mathcal{N}}$, with

$$Y_k(T) = \frac{\langle (\vec{\Delta}(T) \cdot \hat{\psi}_k)^2 \rangle_t}{\sum_{k'} \langle (\vec{\Delta}(T) \cdot \hat{\psi}_{k'})^2 \rangle_t} \quad (2)$$

where $\{\vec{\Delta}(T)\} = \{\vec{r}(T)\} - \{\vec{R}\}$ is the $3N$ -dimensional deviation of the protein structure from the native fold configuration projected onto the NMs, and averaged both over time $\langle \dots \rangle_t$ and over \mathcal{N} different initial conditions drawn from the same equilibrium distribution at temperature T , $\langle \dots \rangle_{\mathcal{N}}$. We have explicitly verified that the two averages commute, so as to strengthen the statistical significance of the sampling and averaging procedures. Statistical uncertainties were computed as the standard errors on the realization averages $\Delta\Theta_k(T) = \sqrt{[\langle Y_k^2(T) \rangle_{\mathcal{N}} - \langle Y_k(T) \rangle_{\mathcal{N}}^2] / \mathcal{N}}$.

Protein trajectories are calculated within the isokinetic scheme [10], which provides a correct sampling of the configuration space [19]. Forces are calculated using the coarse-grained Gō model introduced in Ref. 11 where each amino-acid is replaced by a bead with the average amino-acid mass, whose equilibrium position coincides with that of its α -carbon. Successive beads along the chain are connected by stiff harmonic springs, mimicking the peptide bond and maintaining the chain connectivity. In line with native-centric schemes, non-bonded interactions between non consecutive α -carbons are modelled with Lennard-Jones 12-10 potentials if the atoms are in contact in the native state according to a given interaction cutoff R_c and with purely repulsive interactions otherwise. The parameters of the non-bonded interactions are fixed as $R_c = 6.5 \text{ \AA}$ and $R_c = 7.5 \text{ \AA}$ for $N \leq 100$ and $N > 100$ respectively. The force field is completed by standard harmonic angle-bending interactions, plus the

dihedral potential energy

$$V_{dh} = \sum_{i=3}^{N-2} k_{\phi}^{(1)} [1 - \cos(\Delta\phi_i)] + k_{\phi}^{(3)} [1 - \cos 3(\Delta\phi_i)] \quad (3)$$

where $\Delta\phi_i$ are the the dihedral angle deviations from the native values [20]. Normal modes are computed from the dynamical matrix of the Gō model, according to equation (1), after a conjugate-gradient relaxation of the PDB structures, necessary so to obtain the true minimum of the model potential [21].

In order to locate the unfolding temperatures, we have performed thermal unfolding simulations coupled to multiple histogram reconstructions [12] of the specific heat.

We have analyzed a number of protein structures [22], ranging in length from $N = 57$ to $N = 171$ and heterogeneous for α and β content. The first notable finding is that a restricted number of low-frequency normal modes is always able to capture a sizable fraction of the equilibrium fluctuations over a broad temperature range, from $T = 0$ to about 10-20 % below T_f . This is clearly represented in Fig.2 showing the behavior of the first ten TICs of Lysozyme and of OMPR DNA-binding domain. The TICs of Lysozyme, after a major rearrangement close to $T = 0$, appear strikingly robust over the whole range where the protein structure is stable, while those of the DNA-binding domain fluctuate wildly. Remarkably, in the latter structure, the mode whose TIC is the most important at intermediate temperatures gave nearly no contribution to fluctuations close to the native minimum. Conversely, the NMs that captured the $T \approx 0$ fluctuations appear to swap and rapidly lose spectral weight as temperature increases. Note that the first TICs of Lysozyme fall off much closer to T_f than those of the DNA-binding domain (see values of T_f in the caption). These results manifestly warn on the use

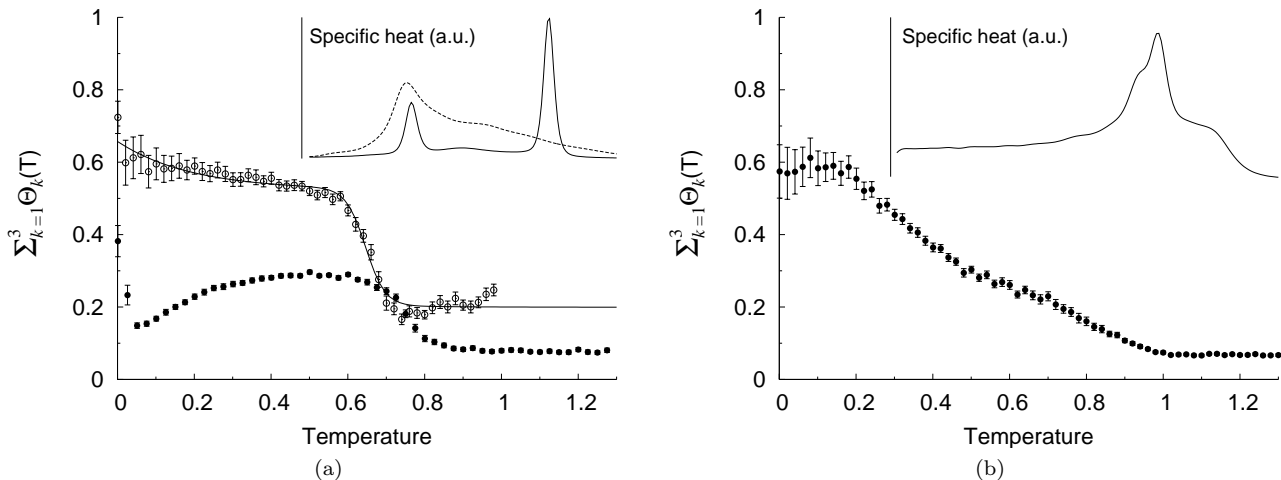


FIG. 3: Cumulative involvement coefficient over the first three modes for: (a) Lysozyme, $N = 162$, PDB code 166L (empty circles) and a surrogate self-avoiding polymer occupying the same volume (filled circles) and (b) the peptide-binding fragment from Hsp40 (b), $N = 171$, PDB code HDJ1. Insets: specific heat (unfolding) on the same temperature scale. In panel (a): wild type molecule (dashed line) and the surrogate (solid line).

of single-mode reconstructions of conformational changes using zero-temperature NMs, as these are not guaranteed to provide stable spectral measures at physiological temperatures. Indeed the individual low-frequency TICs are observed to fluctuate substantially, or even exchange spectral weight among each others, with respect to zero temperature before stabilizing.

Despite the observed fluctuations of TIC values at low and intermediate temperatures, a global measure gathering the contributions from several low-frequency NMs appears to be a more stable indicator of spectral weight over the whole thermal span (see Figs. 2 (b) and 3) for all analyzed structures. Note that this is also the case for the wildly fluctuating TICs of the OMPR DNA-binding domain (see again Fig. 2 (b)), when the first three of them are aggregated. Hence, subspace-based, rather than single-mode-based reconstructions carry the relevant spectral weight. Incidentally, this sheds further light on the observed correlation between low-frequency subspaces of NMs and essential modes pointed out in Ref. 13.

As T_f is approached, a transition of variable width to equipartition is invariably observed. Above T_f , TICs are no longer sensitive to structural rearrangements. However, the nature of such transitions appears rooted in the special structural features of proteins. More precisely, TICs may relax to equipartition more or less abruptly. In this regard, crucial issues seem to be (i) the degree of structural arrangement at the secondary level and (ii) deviations from globularity of the scaffold.

(i) To address the first point, we generated for a few structures self-avoiding polymers of the same length as the corresponding proteins and confined in the same enveloping ellipsoid as calculated through the correspond-

ing inertial tensor. The necessary excluded volume constraints and local persistence length properties were imposed by requiring that the three-body radii be never lower than 2.7 \AA , as described in Ref. 14. By doing so, the ensuing structures show the same internal static two- and three-body correlations as the original proteins, while almost lacking the distinctive occurrence of α and β motifs. As shown in Fig. 3(a), NMs of such surrogate structures do not capture the dynamical fluctuations to the same extent as in the original proteins. This has been verified for different proteins in our ensemble. Hence, we reaffirm the principle that functional motions that can be captured through NM analysis are rooted in the special arrangements of protein folds [9, 15, 16, 17]. This is the second important point we wish to stress.

(ii) Not all proteins possess globular folds, some DNA- and peptide-binding fragments, for example, being characterized by less regular shapes, necessary to adapt to their targets upon binding. This, in turn, implies a varying degree of structure-related cooperativity in the dynamics. Therefore, it is instructive to assess the impact of deviations from globularity on the temperature trend of TICs in such cases. In Fig. 3(b), we show that the TICs describing fluctuations of the human Hsp40 peptide-binding fragment, a strongly non-globular protein (see cartoon in Fig. 1), are indeed characterized by a weak degree of cooperativity. In particular, it is clear that they no longer represent a faithful measure of the overall dynamics already well below T_f .

Finally, to highlight the role of the energy landscape features on the temperature dependence of TICs, we have analyzed F1-ATPase, a globular protein with a high content of α and β motifs. Fig. 4 shows the TIC thermal plot computed both with the full potential and by

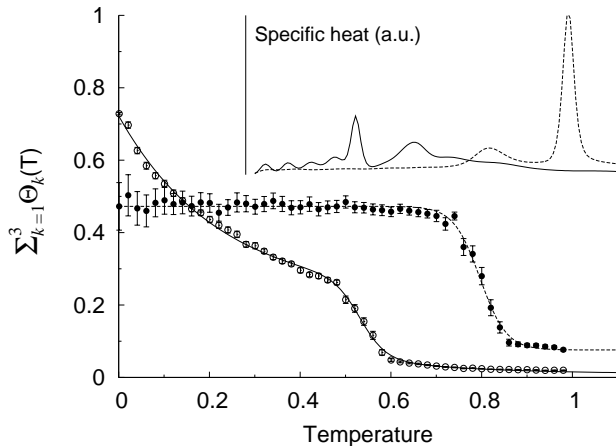


FIG. 4: Cumulative involvement coefficient over the first three modes for the ϵ -subunit of the F1-ATPase ($N = 138$, PDB code 1BSN) computed with the full potential (filled circles) and without dihedral forces (empty circles). Lines are just guides to the eye. Inset: specific heat (unfolding) for the full model (dashed line) and without dihedral terms (solid line) on the same temperature scale.

switching off the dihedral terms (3), which are essential in order to reproduce the cooperativity of protein folding thermodynamics within a $G\bar{o}$ scheme [18]. Since it is also known that less globular proteins are less cooperative, we expect that, due to the lack of the dihedral term, TICs will also be affected, showing a behavior similar to what observed for non-globular proteins such as HDJ1. Indeed, Fig. 4 documents the validity of our inference. Note that the strong cooperativity and thermal resilience of TICs are both profoundly eroded starting from relatively small temperatures. This completes the series of our findings.

In this Letter we have shown that sizable values and thermal resilience of TICs are deeply rooted in the presence of secondary motifs and in the degree of their packing within protein scaffolds. The fluctuations of more irregular, less compact and less cooperative proteins are manifestly harder to capture through normal modes. Although our results confirm the validity of NM analysis of protein functional motions, we have shown that subspaces, typically spanned by the first few low-frequency modes, rather than single normal modes, ought to be considered as identifying the relevant functional motions. This conclusion stems in a clear fashion from the observation that the *spectral capacity* of individual modes, as measured through TICs, often differs substantially at physiological temperatures with respect to the traditional static involvement coefficients at zero-temperature. Moreover, we have brought to the fore

a crucial *liaison* between the meaningfulness of a NM-based description of functional fluctuations at physiological temperatures and the degree of cooperativity of proteins.

The authors wish to thank Bingdong Sha for making the HDJ1 structure available prior to publication.

-
- [1] I. Bahar and A. J. Rader, *Current Opinion in Structural Biology* **15**, 586 (2005).
 - [2] D. Case, *Current Opinion in Structural Biology* **4**, 285 (1994).
 - [3] N. Go, T. Noguti, and T. Nishikawa, *Proceedings of the National Academy of Sciences* **80**, 3696 (1983).
 - [4] B. Brooks and M. Karplus, *Proc Natl Acad Sci U S A* **80**, 6571 (1983 Nov), ISSN 0027-8424 (Print).
 - [5] M. M. Tirion, *Physical Review Letters* **77**, 1905 (1996).
 - [6] A. R. Atilgan, S. R. Durell, R. L. Jernigan, M. C. Demirel, O. Keskin, and I. Bahar, *Biophysical Journal* **80**, 505 (2001).
 - [7] A. Amadei, A. Linssen, and H. Berendsen, *Proteins* **17**, 412 (1993).
 - [8] M. Balsara, W. Wriggers, Y. Oono, and K. Schulten, *Journal of Physical Chemistry* **100**, 2567 (1996).
 - [9] P. De Los Rios, F. Cecconi, A. Pretre, G. Dietler, O. Michielin, F. Piazza, and B. Juanico, *Biophys. J.* **89**, 14 (2005).
 - [10] G. P. Morriss and C. P. Dettmann, *Chaos* **8**, 321 (1998).
 - [11] C. Clementi, H. Nymeyer, and J. Onuchic, *Journal of Molecular Biology* **298**, 937 (2000).
 - [12] A. M. Ferrenberg and R. H. Swendsen, *Phys. Rev. Lett.* **61**, 2635 (1988).
 - [13] C. Micheletti, P. Carloni, and A. Maritan, *Proteins - Structure Function and Bioinformatics* **55**, 635 (2004).
 - [14] J. R. Banavar, A. Flammini, D. Marenduzzo, A. Maritan, and A. Trovato, *Complexus* **1**, 4 (2003).
 - [15] F. Tama and Y. H. Sanejouand, *Protein Engineering Design and Selection* **14**, 1 (2001).
 - [16] C. Chennubhotla, A. J. Rader, L. W. Yang, and I. Bahar, *Physical Biology* **2**, S173 (2005).
 - [17] F. Tama and C. Brooks, *Annu Rev Biophys Biomol Struct* **35**, 115 (2006).
 - [18] M. Knott, H. Kaya, and H. S. Chan, *Polymer* **45**, 623 (2004).
 - [19] Since the isokinetic scheme conserves both linear and angular momenta, no special alignment procedure is needed before computing conformational changes, if care is taken to set both total momenta to zero at the beginning of each simulation run.
 - [20] The dihedral angle at site i is defined by the two adjacent planes formed by the four consecutive C_α 's at $i-2$, $i-1$, i , $i+1$.
 - [21] Codes available from the authors upon request.
 - [22] PDB codes: 166L, 1FAS, 1OOI, HDJ1, 1BFE, 1BSN, 1CHN, 1FVQ, 1OPC, 1AWO, 1TIT, 1UBI, 1NEB.